Social Cognitive and Affective Neuroscience, 2025, **20**(1), nsaf018

DOI: https://doi.org/10.1093/scan/nsaf018
Advance Access Publication Date: 8 March 2025
Original Research & Neuroscience

Connectome-wide brain signature during fast-food advertisement exposure predicts BMI at 2 years

Afroditi Papantoni[1,2], Ashley N. Gearhardt[3], Sonja Yokum[4], Lindzey V. Hoover[3], Emily S. Finn[5], Grace E. Shearrer[6], Lindsey Smith Taillie[1], Saame Raza Shaikh[1], Katie A. Meyer[1], Kyle S. Burger[1,2,7,*]

[1]Department of Nutrition, Gillings School of Global Public Health, University of North Carolina at Chapel Hill, Chapel Hill, NC 27599, United States
[2]Monell Chemical Senses Center, Philadelphia, PA 19104, United States
[3]Department of Psychology, University of Michigan, Ann Arbor, MI 48109, United States
[4]Oregon Research Institute, Springfield, OR 97477, United States
[5]Department of Psychological and Brain Sciences, Dartmouth College, Hanover, NH 03755, United States
[6]Department of Family and Consumer Sciences, University of Wyoming, Laramie, WY 82071, United States
[7]Biomedical Research Imaging Center, University of North Carolina, Chapel Hill, NC 27514, United States
[*]Corresponding author. Monell Chemical Senses Center, 3500 Market St, Philadelphia, PA 19104, United States. E-mail: kburger@monell.org

Abstract

Food advertisements target adolescents, contributing to weight gain and obesity. However, whether brain connectivity during those food advertisements can predict weight gain is unknown. Here, 121 adolescents [14.1 ± 1.0 years; 50.4% female; body mass index (BMI): 23.4 ± 4.8; 71.9% White] completed both a baseline fMRI paradigm viewing advertisements (unhealthy fast food, healthier fast food, and nonfood) and an anthropometric assessment 2 years later. We used connectome-based predictive modeling to derive brain networks that were associated with BMI both at baseline and the 2-year follow-up. During exposure to unhealthy fast-food commercials, we identified a brain network comprising high-degree nodes in the hippocampus, parahippocampal gyrus, and fusiform gyrus rich with connections to prefrontal and occipital nodes that predicted lower BMI at the 2-year follow-up ($r = 0.17$; $P = .031$). A similar network was derived from baseline BMI ($n = 168$; $r = 0.34$; $P < .001$). Functional connectivity networks during exposure to the healthier fast food ($P = .152$) and nonfood commercials ($P = .117$) were not significant predictors of 2-year BMI. Key brain regions in our derived networks have been previously shown to encode aspects of memory formation, visual processing, and self-control. As such, the integration of these regions may reflect a mechanism of adolescents' ability to exert self-control toward obesogenic food stimuli.

Keywords: food advertising; fast food; adolescents; CPM; functional connectivity; obesity

Introduction

Adolescents are one of the primary targets of the food marketing industry (Truman and Elliott 2019). The advertisement of unhealthy foods to adolescents has been associated with higher liking of the advertised products, increased fast-food intake, poor diet quality, and greater rates of obesity (Folkvord et al. 2016, Harris et al. 2022, Bagnato et al. 2023). Fast-food companies are among the top advertisers to adolescents with the majority of advertisements in this age group promoting unhealthy fast-food products (Kelly et al. 2019, Pauzé and Potvin Kent 2021). US adolescents are exposed to an average of 9.4 food-related TV ads per day, summing to over 3500 food-related ad views per year (Frazier and Harris 2018). Moreover, adolescents are constantly exposed to food marketing campaigns through social media with 6.2 million adolescents following 27 of the most highly advertised fast-food, snack, and drink brands in 2019 on various social media platforms (Rummo et al. 2020).

Food commercials have the power to influence adolescents' eating behavior via a series of psychological and physiological responses that render food advertisements highly reinforcing, leading to increased food intake (Folkvord et al. 2016), potentially by influencing reward-related networks in the developing brain (Casey and Jones 2010). Two meta-analyses have concluded that acute exposure to unhealthy food advertising significantly increases food intake in children and adolescents (Boyland et al. 2016, Russell et al. 2019). In addition to behavioral observational studies, functional magnetic resonance imaging (fMRI) studies have examined how brain responses can predict behaviors, offering insights into the neural basis of eating behaviors (Giuliani et al. 2018). Exposure to food vs. nonfood commercials is associated with greater brain responses in regions including the cerebellar culmen, middle occipital gyrus, and superior parietal lobule, which are commonly activated in response to both natural (food and sex) and drug cues highlighting their role in reward

Received: 6 June 2024; **Revised**: 26 October 2024; **Accepted**: 5 March 2025

processing, emotional responses, and habit formation (Noori et al. 2016, Yeung 2021). Additionally, exposure to dynamic food commercials, compared to static food ads, elicits greater blood-oxygen-level-dependent (BOLD) response in regions that encode aspects of reward and gustatory processes (ventral tegmental area, substantia nigra, amygdala, and insula), suggesting that a more naturalistic presentation of food cues, as the ones seen in TV ads, might have a greater impact in engaging dopaminergic reward pathways (Yeum et al. 2023). These brain regions are thought to underlie hedonically motivated food behaviors such as food cravings, food-approach behaviors, and appetitive motivation in both animal and human research (Nummenmaa et al. 2012, Siep et al. 2012, Dietrich et al. 2016, Douglass et al. 2017). In support, a cross-sectional analysis of the data in the current sample demonstrated that greater BOLD activation in reward-related regions (nucleus accumbens and caudate) in response to both unhealthy and healthier fast-food vs. nonfood commercials is associated with greater food intake (Gearhardt et al. 2020). Furthermore, less activation in the bilateral fusiform gyrus to both food and nonfood brands (vs. control images) is associated with greater energy intake from branded meals (Masterson et al. 2019). These results suggest that brain responses to branding in general, and not just food brands, could be associated with the energy intake-promoting effects of marketing.

Despite these advances in knowledge, prospective investigations of the impact of food and nonfood commercials on future weight change among adolescents are lacking. Adolescence is a critical developmental period marked by extensive changes in the structure and function of the adolescent brain that refine higher-order cognitive functions including decision-making (Blakemore and Mills 2014, Larsen and Luna 2018). Thus, understanding how exposure to environmental food cues interacts with functional brain connectivity during this sensitive period can provide insight into the brain pathways through which food ad exposure leads to increased food intake and weight gain in adolescents. Advances in fMRI data-driven machine learning-based connectivity analyses have yielded tools, e.g., connectome-based predictive modeling (CPM), that allow us to identify brain circuits predictive of certain behaviors and traits across individuals to develop models of brain–behavior relationships "i.e., neural signatures" (Finn et al. 2015, Rosenberg et al. 2016, Shen et al. 2017). The ability to identify brain functional connectivity patterns that make some adolescents more susceptible to food advertising content than others could ultimately aid in the development of policies that tightly regulate advertisment exposure among the younger population.

Here, we utilized CPM to examine whether functional connectivity networks during passive viewing of food and nonfood advertisements could be derived from baseline body mass index (BMI) and predict future BMI in adolescents. Based on previous work studying BOLD responses to food commercials (Gearhardt et al. 2014, 2020, Masterson et al. 2019, Arrona-Cardoza et al. 2022, Yeum et al. 2023), we hypothesized that increased functional connectivity between regions in dopaminergic networks (dorsal striatum, ventral striatum, and thalamus) and salience networks (insula and amygdala) in response to fast-food commercials compared to nonfood commercials would predict greater BMI in adolescents at a 2-year follow-up.

Materials and methods

Sample

The current sample was drawn from a larger study detailed here (Gearhardt et al. 2020, Hoover 2022). In brief, participants ($n = 193$) were recruited from southeast Michigan between 2015 and 2017 and asked to complete an fMRI task measuring BOLD responses to fast-food (unhealthy and healthier) and nonfood commercials at baseline, and complete height and weight measurements at baseline and the 2-year follow-up. Participants were English-speaking adolescents between 13 and 16 years of age. Adolescents were excluded if they were using psychotropic medications or illicit drugs, had a lifetime psychiatric disorder, a BMI percentile of <5%, or fMRI contraindicators (e.g., presence of metal implants). Of the 193 adolescents in the full sample at baseline, 186 completed the fMRI scan, of which 9 showed excessive movement (i.e., head motion of >3 mm or degrees in any direction within two or more runs), 2 had scan data with acquisition errors, and 2 did not have the correct onset timing files for the fMRI task, resulting in a baseline sample of 173 ($n = 124$ with the 2-year follow-up). Anthropometric measurements for five participants from baseline and three from the 2-year follow-up were flagged as statistical outliers and removed, resulting in a final analytic sample of 168 adolescents at baseline and 121 at the 2-year follow-up.

Overview of study procedures

During the baseline assessment, parents provided written informed consent. Adolescents had their height and weight measured and completed the fMRI commercials neuroimaging paradigm. Adolescents completed a 2 -year follow-up visit, where they repeated the height and weight measurements. Study procedures were approved by the University of Michigan Institutional Review Board.

Measures

Anthropometrics

Participants' height and weight were collected in light clothing without jackets, socks, or shoes. Height was measured using an O'Leary Acrylic Stadiometer (in centimeters, to the nearest tenth); weight was measured using a Detecto Portable Scale (in kilograms, to the nearest tenth). Height and weight measurements were repeated twice and the averages were used for subsequent analyses. BMI values (kg/m^2) were calculated at baseline and the 2-year follow-up. Participants reported their pubertal development at baseline and follow-up using a series of sex-specific line drawings at various stages of pubertal development (Bonat et al. 2002).

Scan procedures

For the fMRI scan, participants were asked to refrain from eating or drinking (except water) following their last meal before the scan (last meal consumed 1–7 h prior to scan). Participants rated their hunger on a scale from 0 (not hungry at all) to 100 (extremely hungry) before the scan. As described in Gearhardt et al. (2020), if a rating of ≥70 was indicated, participants were offered a small snack (e.g., crackers, fruits) to normalize their hunger to a neutral state. From the individuals included in the baseline analysis ($n = 168$), a total of 7.7% received a snack ($n = 13$). From the individuals included in the 2-year follow-up analysis ($n = 121$), a total of 5.8% received a snack ($n = 7$). Hunger ratings were repeated after the snack and hunger was decreased by 53.6% in those who consumed the snack.

fMRI data acquisition

Data were acquired with a GE Discovery MR750 3T scanner. An 8-channel head coil was used to acquire data from the entire brain. Functional data were acquired using a spiral sequence with the following parameters: repetition time (TR) = 2000 ms, echo time (TE) = 30 ms, flip angle = 90°, field of view (FOV) = 22 × 22 cm^2, acquisition matrix 64 × 64, 3-mm slice thickness with no gap, 43

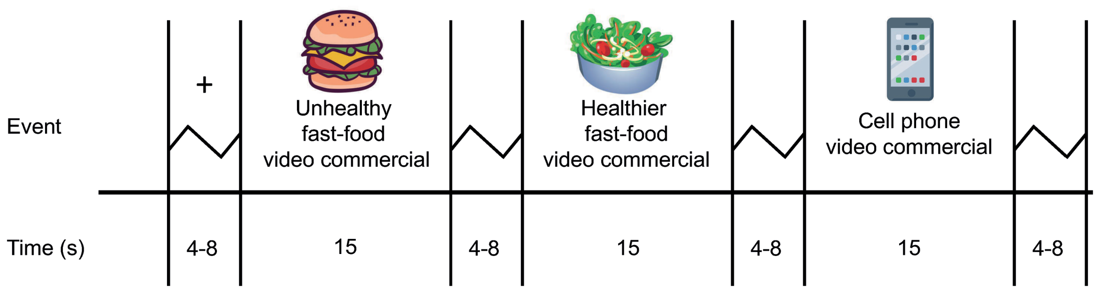

Figure 1. fMRI commercials paradigm.

axial slices, and voxel size = 3.44 × 3.44 × 3.0 mm^3. In total, 156 volumes were collected during each of four functional runs. Anatomical scans were acquired using a high-resolution T1-weighted spoiled-gradient-recalled acquisition (TR = 12.3 ms; TE = 5.2 ms, inversion time (TI) = 500 ms, flip angle = 15°, FOV = 22 × 22 cm^2, slice thickness = 1.0 mm, voxel size = 1 × 1 × 1 mm^3).

fMRI commercial paradigm

The fMRI commercial paradigm was developed to include commercials commonly viewed by young adolescents based on Nielsen Gross Ratings Point national data (Harris 2013). Details on the commercial selection as well as a full list of the commercials used can be found in Gearhardt et al. (2020). Briefly, the stimuli in the fMRI task included 20 fast-food commercials promoting unhealthy food from Wendy's and McDonald's (e.g., Quarter Pounder with Cheese), 20 fast-food commercials for healthier food options from McDonald's and Wendy's (e.g., Southwest Salad), and 20 nonfood phone (control) commercials from AT&T and Verizon (e.g., iPhone). Foods depicted in the commercials were evaluated as unhealthy or healthier using the Nutrient Profile Index (NPI), a measure of overall nutrition quality used in the UK (Ofcom 2006, Rayner et al. 2009). NPI scores range from 1 to 100 (higher score indicates healthier items), with foods in the unhealthy fast-food commercials averaging 44.05 ± 4.21 and foods in the healthier fast-food commercials averaging 70.20 ± 3.86. Each commercial lasted ∼15 s and was shown only once. Between each commercial was a jittered fixation cross (4–8 s) (Fig. 1). The paradigm consisted of four 7-min runs with 15 commercials per run. The order of commercials was randomized in each of the runs and the order of the four runs was randomized over the participants. Participants were instructed to watch the commercials. After the scan, self-reported liking ratings of the commercials in the paradigm were collected. Participants were asked "How much do you LIKE the following products?" for each of the advertised items (i.e., unhealthy fast-food, healthier fast-food, and phones). Responses were provided on a 5-point scale ranging from Dislike Extremely (1 point) to Like Extremely (5 points). In addition, both at baseline and the 2-year follow-up, participants answered questions about the frequency of visiting Wendy's and McDonald's in a typical week to assess their overall fast-food exposure, with 63.7% and 78.5% of adolescents reporting visiting those restaurants at least once per week at baseline and the 2 year follow-up, respectively.

fMRI preprocessing

Following previous work (Burger and Stice 2013), all images were manually realigned to the anterior commissure - posterior commissure line and skull stripped using the Brain Extraction Tool in the FMRIB Software Library FSL; v5.0.9; FMRIB Analysis Group, Oxford, UK). Neuroimaging data were preprocessed and analyzed primarily using Statistical Parametric Mapping (SPM12, Functional Imaging Laboratory, University College of London) in MATLAB (R2015a; MathWorks, Inc., Natick, MA, USA). Anatomic images were segmented and normalized to Montreal Neurological Institute (MNI) space with the use of the DARTEL toolbox. Anatomical data were coregistered to the mean functional image and segmented into six tissue types using unified segmentation approach (Ashburner and Friston 2005). Functional images were realigned to the mean functional image, coregistered with the anatomic images, normalized to MNI space with the use of DARTEL, and smoothed with an 8-mm full-width at half-maximum isotropic Gaussian kernel. DARTEL was used to create a group anatomical template, transformations from which were applied to warp functional data to the ICBM-152 template supplied with SPM12 (Ashburner 2007). Artifact Detection Tools (http://www.nitrc.org/projects/artifact_detect/) software package was used for automatic detection of spikes and motion in the functional data. Motion parameters (three translations and three rotations) were included as regressors in the design matrix at individual-level analysis. Additionally, functional image volumes where the z-normalized global brain activation exceeded 3 SDs from the mean or showed >1.5 mm of composite movement were flagged as outliers and deweighted during individual-level model estimation.

Statistical analyses

Behavioral analysis

Raw BMI scores were used to assess BMI changes, as they are considered better than BMI-for-age percentiles or BMI z-scores for modeling change over time (Adise et al. 2024). Paired sample t-tests were used to compare BMI across the two timepoints, and repeated measures ANOVA was used to explore biological sex by timepoint differences and differences in the liking ratings by commercial type.

Functional connectivity

Following data preprocessing, we used a whole-brain functional atlas defined on a separate group of healthy adult subjects (Shen et al. 2013) to parcellate the brains of each subject into 268 regions of interest. We chose the Shen 268-node parcellation because it covers the whole brain, including subcortical areas and cerebellum, and has been used in previous CPM studies (Rosenberg et al. 2016, Yip et al. 2019, Farruggia et al. 2020, Finn and Bandettini 2021). Here, the mean timecourses per run per participant (i.e., average BOLD signal of all voxels within the node during each task run) for each of the 268 nodes were extracted using Nipype 1.8.6 implemented in Python 3.11.2. To minimize the impact of task-induced co-activation in the functional connectivity analyses (Cole et al. 2019) and capture mostly "background" fluctuations in brain activity induced by the different commercial types, after modeling the task effects within a general linear model design, we extracted the timecourses on the residuals of this regression (Al-Aidroos et al. 2012). Timecourses were concatenated across all available runs per participant, standardized within subject, and detrended to remove linear trends from the signal. Functional connectivity matrices for each subject were created by correlating each node's timecourse with every other node's timecourse to construct 238 × 238 matrices, one per subject (all 30 nodes that were part of the cerebellar canonical network, as defined by Noble et al. (2017) and Greene et al. (2018), were dropped to focus the analyses on networks more commonly associated with BMI; note that 28 nodes in the cerebellum that were part of the other canonical networks were kept in). Correlation coefficients in the 238 × 238 connectivity matrices were transformed to z-scores using Fisher's transformation.

Connectome-based predictive modeling

CPM is a data-driven approach that uses whole-brain functional connectivity to develop models of brain–behavior relationships using machine learning (Finn et al. 2015, Shen et al. 2017). CPM analysis was conducted using previously validated custom scripts in MATLAB (Shen et al. 2017, Boyle and Weng 2023). A detailed description of the CPM protocol can be found in Shen et al. (2017). An overview of the method is as follows:

(i) Without any prior scaling or standardization, data, comprising each subject's functional connectivity matrix and the target behavioral variable, were divided into training and test sets for 10-fold cross-validation, where the total number of subjects was binned into 10 equal size groups, and for each iteration subjects from nine bins (90% of the participants) were used for training and subjects from the one left-out independent bin (10% of participants) were used for testing. We ran two separate models each with a different target variable: one with baseline BMI and the other with 2-year BMI (controlling for baseline BMI). For each model, we then repeated the 10-fold cross-validation process 100 times to create a distribution of the test statistic and ensure its stability across different train-test folds.

(ii) For each model, in the training set, each edge in the connectivity matrix was correlated with the target variable. Target variables (baseline BMI, 2-year BMI) were normally distributed, and thus we used partial Pearson's correlation to control for age, biological sex, baseline pubertal stage for both models, and baseline BMI for the 2-year BMI model only. In *post hoc* analyses, additional covariates (pre-scan snack intake, pre-scan hunger ratings, self-reported liking ratings for the commercials, change in pubertal stage from baseline to the 2-year follow-up, and fast-food exposure) were included in the models but results remained similar in statistical significance across all models and types of commercials, so they were omitted from the results presented here.

(iii) A feature selection threshold was applied to select the most relevant edges for use in the predictive model based on the correlation coefficients calculated in (ii). Here, we retained edges with $|r| > 0.25$ (corresponding to a two-tailed *P*-value of approximately .006) for the correlation between connectivity and the target variable. Edges were separated into a positive network (edges where connectivity is positively correlated with the target variable) and a negative network (edges where connectivity is negatively correlated with the target variable).

(iv) For each subject in the training set, we calculated the summed connectivity strength across all retained edges in the positive and negative networks separately.

(v) Still using the training set only, we fitted two linear models: one using the positive network and the other using the negative network, by regressing network strength on the target variable. The model parameters were extracted and saved.

(vi) For each subject in the test set, we calculated positive and negative network strength using the same method described in (iii). These values were used as input to each of the linear models estimated in (v) to create the predicted scores for the target variable for each subject.

Evaluating model performance and statistical significance

To assess prediction accuracy of each linear model (positive and negative), we correlated the predicted (model generated) and observed target variable scores across subjects using Pearson's correlation. The coefficient of determination (r^2) was also calculated using the sum-of-squares approach to assess the proportion of variance in the observed values explained by the predicted values. Given that correlation is a relative measure of accuracy rather than an absolute one, the mean absolute error (MAE) between the predicted and observed target variable scores was also calculated and reported below.

In cross-validation, regression folds are not independent of one another, and as such, we used nonparametric permutation testing to assess the statistical significance of prediction accuracy. We generated a null distribution for the correlations between the predicted and observed target variable scores by randomly shuffling the target variable with respect to connectivity matrices and repeating the entire CPM pipeline 10 000 times. The nonparametric *P*-value for each network strength was calculated as the proportion of permuted correlation coefficients (i.e., from the null distribution) that are greater than or equal to the true prediction correlation coefficient (i.e., mean across the 100 true models) for that network strength model.

Data visualization

Only edges selected in at least 90% of all folds across all 100 iterations were extracted and graphed for the significant networks. Figures were constructed using BioImage Suite (Joshi et al. 2011). The 238 nodes included in the analyses were assigned to nine canonical networks as defined in Greene et al. (2018) emphasizing different properties of the human brain and consist of medial-frontal (MF), fronto-parietal (FP), default mode network (DMN), motor/somatosensory (Mot), primary visual (VI), secondary visual (VII), visual association (VAs), salience (SAL), and subcortical (SC) networks.

Results

Participant characteristics at baseline ($n = 168$) and the 2-year follow-up ($n = 121$) are summarized in Table 1. The subsample that did not complete the 2-year follow-up ($n = 47$) was significantly older at baseline compared to the participants that completed the 2-year follow-up ($t = 2.70$, $P = .008$), but showed no other differences.

BMI was significantly higher at the 2-year follow-up compared to baseline [$t(121) = 6.53$, $P < .001$]. Differences among self-reported liking of the three types of advertised items were observed [$F(2, 334) = 33.74$, $P < .001$]; nonfood (phone) items

Table 1. Participant characteristics.

	Baseline				Two-year follow-up	
	$n=168$		$n=121$		$n=121$	
	Count (percent)					
Sex						
Female	86 (51.2)		61 (50.4)			
Male	82 (48.8)		60 (49.6)			
Ethnicity						
Hispanic or Latino	15 (8.9)		13 (10.7)			
Not Hispanic or Latino	153 (91.1)		108 (89.3)			
Race						
American Indian/Alaska Native	3 (1.8)		3 (2.5)			
Asian	2 (1.2)		1 (0.8)			
Black or African American	22 (13.1)		12 (9.9)			
White	118 (70.2)		87 (71.9)			
More than one race	14 (8.3)		11 (9.1)			
Other/unknown	9 (5.4)		7 (5.8)			
Weight category						
Underweight	0 (0)		0 (0)		1 (0.8)	
Healthy weight	94 (56.0)		72 (59.5)		68 (56.2)	
Overweight	39 (23.2)		23 (19.0)		27 (22.3)	
Obese	35 (20.8)		26 (21.5)		25 (20.7)	
Pubertal (tanner) pubic hair stage	Girls ($n=86$)	Boys ($n=81$)[a]	Girls ($n=61$)	Boys ($n=60$)	Girls ($n=60$)[a]	Boys ($n=60$)
1	0 (0)	0 (0)	0 (0)	0 (0)	0 (0)	0 (0)
2	2 (2.3)	5 (6.2)	1 (1.6)	5 (8.3)	0 (0)	0 (0)
3	8 (9.3)	21 (25.9)	7 (11.5)	14 (23.3)	2 (3.3)	2 (3.3)
4	36 (41.9)	33 (40.7)	25 (41.0)	25 (41.7)	21 (35.0)	24 (40.0)
5	40 (46.5)	22 (27.2)	28 (45.9)	16 (26.7)	37 (61.7)	34 (56.7)
Pubertal (tanner) breast stage (girls only)						
1	0 (0)		0 (0)		0 (0)	
2	2 (2.3)	–	1 (1.6)	–	0 (0)	–
3	23 (26.7)		16 (26.2)		2 (3.3)	
4	37 (43.0)		27 (44.3)		27 (45.0)	
5	24 (27.9)		17 (27.9)		31 (51.7)	
	Mean ± SD					
Age (years)[b]	14.3 (1.0)		14.1 (1.0)		16.1 (1.0)	
BMI (kg/m^2)	23.7 (4.8)		23.4 (4.8)		24.8 (5.1)	
BMI z-score	0.82 (0.90)		0.78 (0.91)		0.75 (0.98)	
Liking ratings for commercials						
Unhealthy fast food[c]	2.84 (0.60)		2.84 (0.62)		–	
Healthier fast food	2.69 (0.59)		2.70 (0.58)		–	
Nonfood phone[d]	3.07 (0.50)		3.09 (0.50)		–	

[a]Pubertal stage was missing for one participant at baseline and one participant at the 2-year follow-up.
[b]Age significantly higher in the full sample ($n=168$ vs. $n=121$) ($P=.008$).
[c]Liking ratings significantly higher for unhealthy vs. healthier fast-food commercials ($P=.001$).
[d]Liking ratings significantly higher for nonfood vs. unhealthy fast-food commercials ($P<.001$) and nonfood vs. healthier fast-food commercials ($P<.001$).

were rated higher compared to both unhealthy and healthier fast-food items ($P<.001$ for both). Unhealthy fast-food items had higher liking ratings than healthier food items ($P=.001$; Table 1).

Pubertal stage at baseline was significantly higher in female vs. male participants at baseline ($\chi^2=12.37$, $P=.006$), but not at the 2-year follow-up ($\chi^2=0.32$, $P=.853$). Pubertal stage was also significantly different by race at baseline (Black adolescents reported higher pubertal stage; $\chi^2=56.56$, $P<.001$), but not at the 2-year follow-up ($\chi^2=13.18$, $P=.356$).

Brain networks in response to unhealthy fast-food commercials

Baseline

We first examined whether functional connectivity in response to each type of commercial is significantly associated with BMI at baseline, controlling for age, sex, and baseline pubertal stage. We identified a functional connectivity network in response to passive viewing of "unhealthy fast-food" commercials where stronger connectivity among the nodes of the network was associated with lower BMI at baseline ($r=0.341$, nonparametric permutation $P<.001$, $r^2=0.116$, MAE $=3.722$; Fig. 2). This "negative" network contained 450 edges (1.6% of all possible connections among the nodes in the atlas used). Highest-degree nodes (i.e. nodes with the greatest number of nodal connections contributing to the network) were found in the fusiform gyrus, cerebellum, occipital cortex, hippocampus, and anterior prefrontal cortex (Table 2). These nodes are summarized based on their overlap with the nine canonical networks and can be seen in Fig. 2b and c. We observed connections within the SC canonical network, as well as connections between the SC and VAs, SAL, and DMN canonical networks.

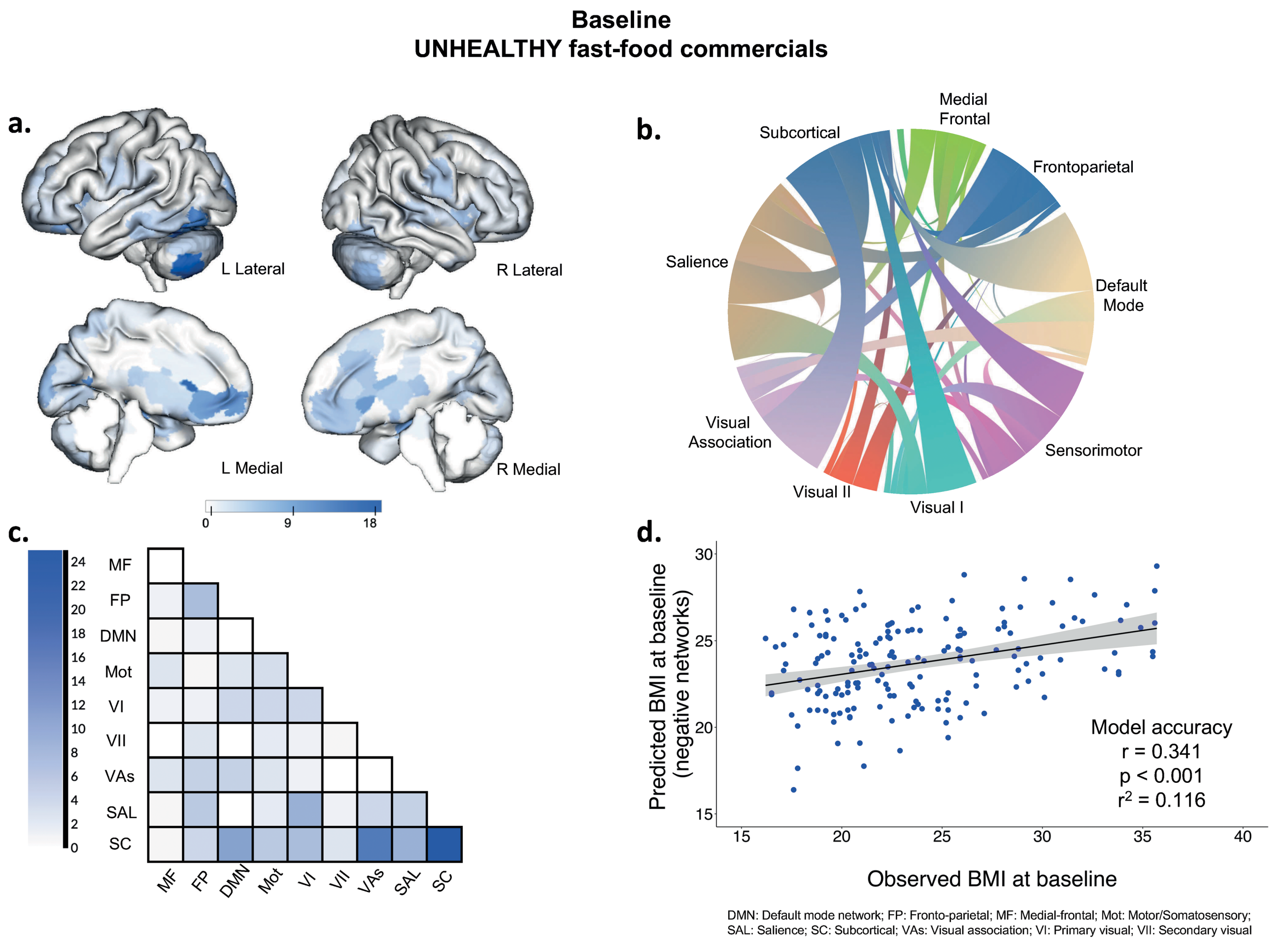

Figure 2. Brain networks associated with baseline BMI during exposure to unhealthy fast-food commercials. Representation of negative BMI networks at baseline in response to the unhealthy fast-food commercials. Greater number of connections between the displayed nodes at baseline is associated with lower baseline BMI. Darker colored regions (a) indicate nodes with a greater number of connections. Chord diagrams (b) represent the connections among the nine canonical brain networks. Matrix cells (c) represent the total number of edges connecting nodes between each network pair among the canonical networks, where darker colors indicate more connections. Scatterplots (d) represent model accuracy, i.e., the relationship between the observed versus the predicted baseline BMI generated by the functional connectivity CPM models during exposure to unhealthy fast-food commercials. Models have been adjusted for age, sex, and baseline pubertal stage. Coefficient of determination (r^2) is calculated as the total sum of squares explained by the model.

Table 2. High-degree nodes (top 5%) in the negative BMI network at baseline for unhealthy fast-food commercials.

Degree	Degree as proportion of network size[a]	Shen 268 atlas node (Shen et al. 2013)	Region	Canonical Network	MNI coordinates (x, y, z)
		Negative network			
18	0.040	200	L Fusiform gyrus	VAs	−43, −52, −17
17	0.038	257	White matter (callosal body)	SC	−11, 24, 10
17	0.038	246	L Cerebellum	FP	−43, −64, −46
12	0.027	206	L Occipital	VAs	−43, −70, −14
11	0.024	216	L Lingual gyrus	VI	−22, −67, 7
10	0.022	232	L Hippocampus	SC	−36, −25, −15
10	0.022	217	White matter (callosal body)	SC	−24, −41, 20
10	0.022	138	L Anterior prefrontal cortex	DMN	−7, 48, −6
10	0.022	123	R Caudate	SC	13, 20, −1
9	0.020	230	L Hippocampus	SC	−32, −40, −4
9	0.020	134	L Orbitofrontal cortex	DMN	−5, 29, −10
9	0.020	94	R Hippocampus	SC	36, −15, −18

[a]Negative network consists of a total of 450 edges.

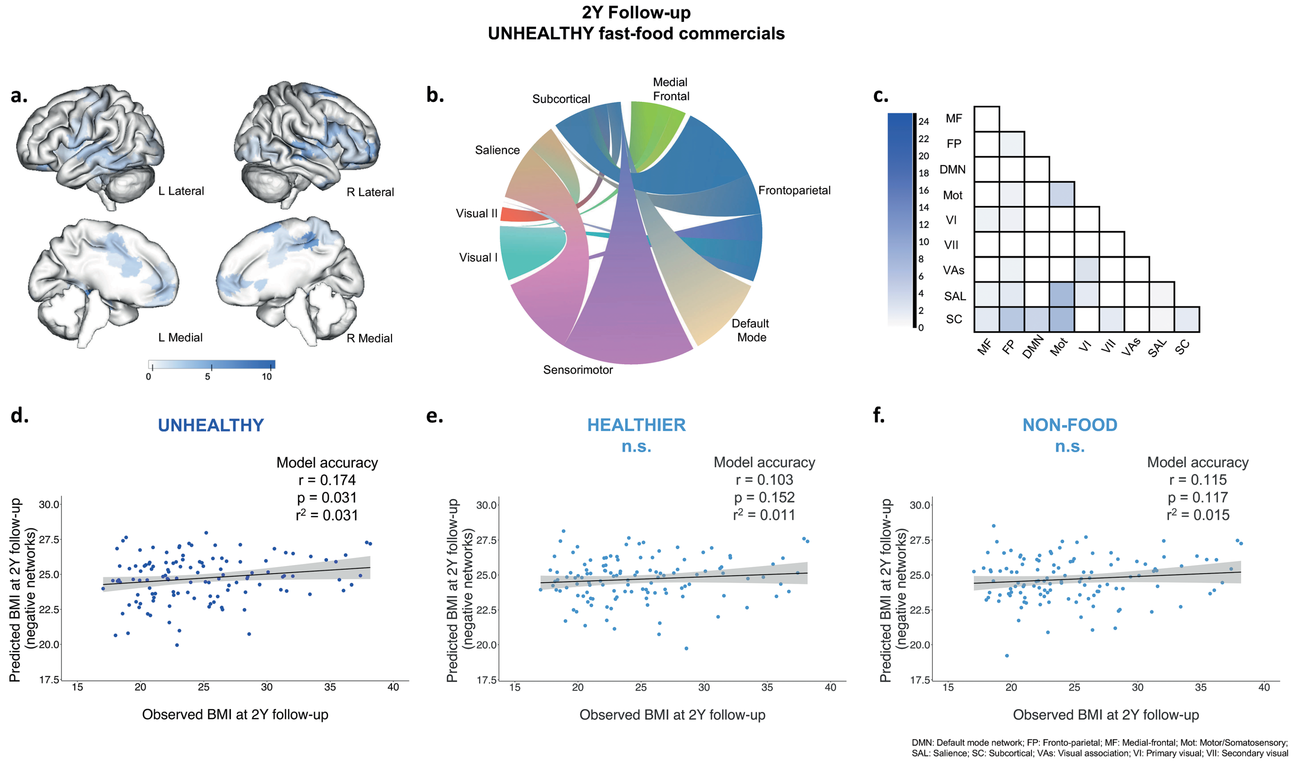

Figure 3. Brain networks predicting lower BMI over 2 years during exposure to unhealthy fast-food commercials. Representation of negative BMI networks at the 2-year follow-up in response to the unhealthy fast-food commercials. Greater number of connections between the displayed nodes at baseline is predictive of lower BMI at the 2-year follow-up. Darker colored regions (a) indicate nodes with a greater number of connections. Chord diagrams (b) represent the connections among the nine canonical brain networks. Matrix cells (c) represent the total number of edges connecting nodes between each network pair among the canonical networks, where darker colors indicate more connections. Scatterplots represent model accuracy, i.e., the relationship between the observed versus the predicted 2-year follow-up BMI generated by the functional connectivity CPM models during exposure to (d) unhealthy fast-food, (e) healthier fast-food, and (f) nonfood phone commercials. Only the CPM based on the unhealthy fast-food functional connectivity reached statistical significance. Models have been adjusted for age, sex, baseline pubertal stage, and baseline BMI. Coefficient of determination (r^2) is calculated as the total sum of squares explained by the model.

Two-year follow-up

We identified a functional connectivity network in response to passive viewing of "unhealthy fast-food" commercials where stronger connectivity among the nodes predicted lower BMI at 2 years ($r = 0.174$, nonparametric permutation $P = .031$, $r^2 = 0.031$, MAE = 4.164; Fig. 3), controlling for age, sex, baseline pubertal stage, and baseline BMI. This network contained 132 edges (0.5% of all possible connections). Highest-degree nodes were found in the parahippocampal gyrus, hippocampus, posterior cingulate cortex, superior temporal gyrus, and insula (Table 3). These nodes are summarized based on their overlap with the nine canonical networks and can be seen in Fig. 3b and c. Here, nodes within the SC canonical network were interconnected with nodes within the MF, FP, DMN, and Mot networks.

Brain networks in response to healthier fast-food commercials

Baseline

A functional connectivity network in response to passive viewing of "healthier fast-food" commercials was identified, where stronger connectivity among the nodes of the network was associated with lower BMI at baseline ($r = 0.366$, nonparametric permutation $P < .001$, $r^2 = 0.134$, MAE = 3.672; Fig. 4), controlling for age, sex, and baseline pubertal stage. This negative network contained 566 edges (2.1% of all possible connections). Highest-degree nodes for the network were found in the fusiform gyrus, cerebellum, occipital cortex, and hippocampus (Table 4). These nodes are summarized based on their overlap with the nine canonical networks and can be seen in Fig. 4b and c. Here, we observed connections within the FP and within the SC canonical networks. There were also connections between the FP, VAs, SAL, and SC networks.

Two-year follow-up

Functional connectivity networks in response to passive viewing of the "healthier fast-food" commercials did not significantly predict BMI at the 2-year follow-up ($r = 0.103$, nonparametric permutation $P = .152$, $r^2 = 0.011$, MAE = 4.194; Fig. 3e), controlling for age, sex, baseline pubertal stage, and baseline BMI.

Brain networks in response to nonfood commercials

Baseline

There was also a significant functional connectivity network in response to passive viewing of "nonfood" commercials where stronger connectivity among the nodes of the network was associated with lower BMI at baseline ($r = 0.331$, nonparametric permutation $P < .001$, $r^2 = 0.110$, MAE = 3.732; Fig. 5), controlling for age, sex, and baseline pubertal stage. This negative network contained 666 edges (2.4% of all possible connections). Highest-degree nodes were found in the fusiform gyrus, cerebellum, and occipital cortex (Table 5). These nodes are summarized based on their overlap with the nine canonical networks and can be seen in Fig. 5b and c. We found connections within the SC and within the Mot networks,

Table 3. High-degree nodes (top 5%) in the network that predicted lower BMI after 2 years during exposure to unhealthy fast-food commercials.

Degree	Degree as proportion of network size[a]	Shen 268 atlas node (Shen et al. 2013)	Region	Canonical network	MNI coordinates (x, y, z)
		Negative network			
10	0.076	95	R Parahippocampal gyrus	SC	28, −29, −14
8	0.061	230	L Hippocampus	SC	−32, −40, −4
7	0.053	233	L Parahippocampal gyrus	SC	−21, −31, −11
5	0.038	91	R Dorsal posterior cingulate cortex	SAL	8, −40, 48
4	0.03	63	R Duperior temporal gyrus	Mot	62, −24, −3
4	0.03	35	R Insula	Mot	41, 4, 7
4	0.03	29	R Supplementary motor area	SAL	14, 6, 65
4	0.03	7	R Anterior prefrontal cortex	FP	31, 55, −4
3	0.023	234	L Parahippocampal gyrus	SC	−31, −24, −27
3	0.023	231	L Hippocampus	SC	−23, −13, −17
3	0.023	198	L Fusiform gyrus	VI	−27, −43, −16
3	0.023	168	L Insula	Mot	−39, 2, 10

[a]Negative network consists of a total of 132 edges.

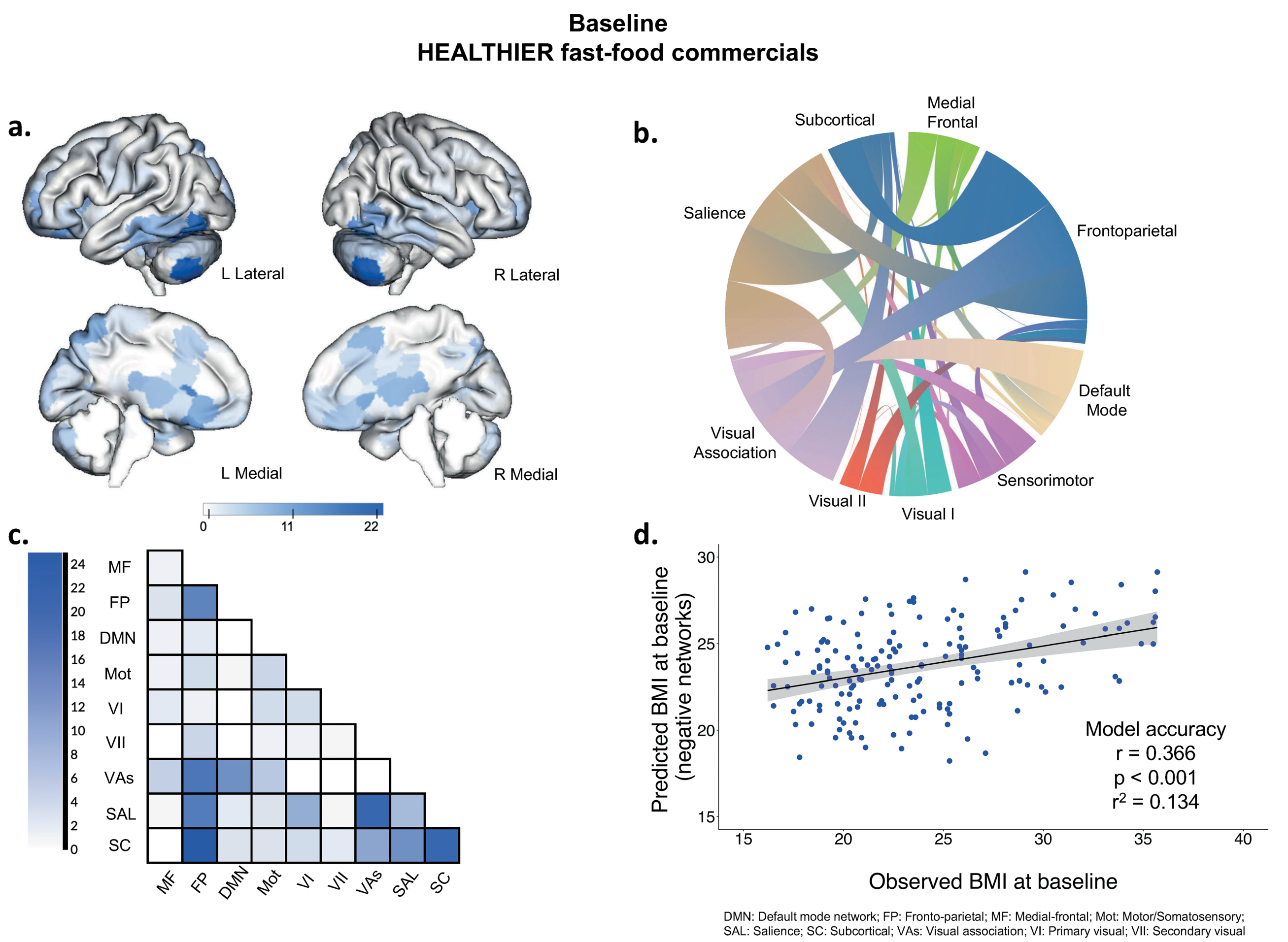

Figure 4. Brain networks associated with baseline BMI during exposure to healthier fast-food commercials. Representation of negative BMI networks at baseline in response to the healthier fast-food commercials. Greater number of connections between the displayed nodes at baseline is associated with lower baseline BMI. Darker colored regions (a) indicate nodes with a greater number of connections. Chord diagrams (b) represent the connections among the nine canonical brain networks. Matrix cells (c) represent the total number of edges connecting nodes between each network pair among the canonical networks, where darker colors indicate more connections. Scatterplots (d) represent the relationship between the observed versus the predicted baseline BMI generated by the CPM model. Models have been adjusted for age, sex, and baseline pubertal stage. Coefficient of determination (r^2) is calculated as the total sum of squares explained by the model.

Table 4. High-degree nodes (top 5%) in the negative BMI network at baseline for healthier fast-food commercials.

Degree	Degree as proportion of network size[a]	Shen 268 atlas node (Shen et al. 2013)	Region	Canonical network	MNI coordinates (x, y, z)
		Negative network			
23	0.041	246	L Cerebellum	FP	−43, −64, −46
22	0.039	200	L Fusiform gyrus	VAs	−43, −52, −17
22	0.039	116	R Cerebellum	FP	42, −64, −49
18	0.032	206	L Occipital	VAs	−43, −70, −14
16	0.028	257	White matter (callosal body)	SC	−11, 24, 10
13	0.023	232	L Hippocampus	SC	−36, −25, −15
13	0.023	67	R Fusiform gyrus	VAs	36, −69, −17
12	0.021	152	L Inferior frontal gyrus	SAL	−28, 36, −16
12	0.021	136	L Orbitofrontal cortex	SAL	−6, 18, −22
10	0.018	123	R Caudate	SC	13, 20, −1
9	0.016	178	L Superior parietal lobule	SAL	−10, −66, 55
9	0.016	142	L Anterior prefrontal cortex	FP	−29, 54, 3

[a]Negative network consists of a total of 566 edges.

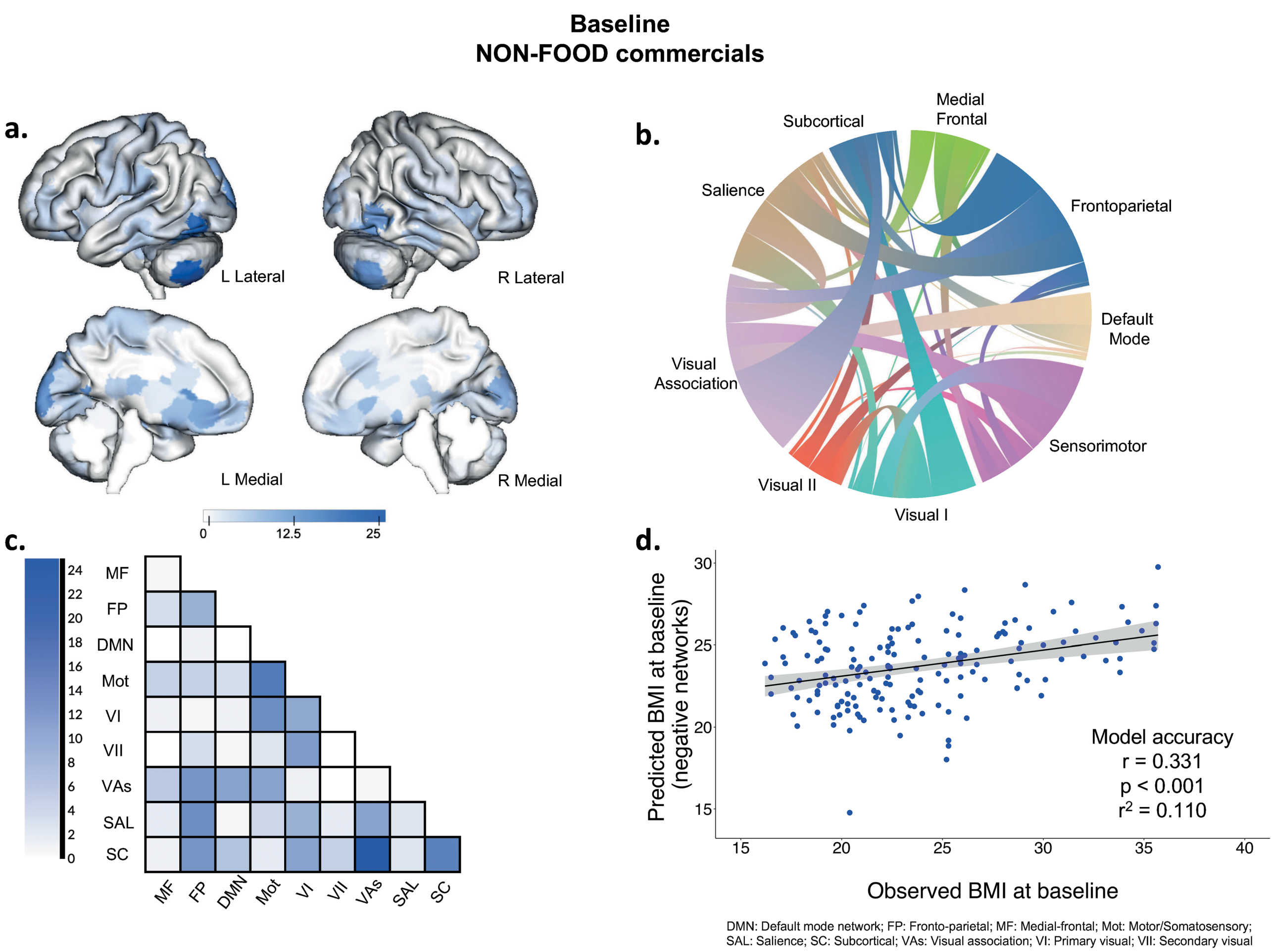

Figure 5. Brain networks associated with baseline BMI during exposure to nonfood commercials. Representation of negative BMI networks at baseline in response to the nonfood commercials. Greater number of connections between the displayed nodes at baseline is associated with lower baseline BMI. Darker colored regions (a) indicate nodes with a greater number of connections. Chord diagrams (b) represent the connections among the nine canonical brain networks. Matrix cells (c) represent the total number of edges connecting nodes between each network pair among the canonical networks, where darker colors indicate more connections. Scatterplots (d) represent the relationship between the observed versus the predicted baseline BMI generated by the CPM models. Models have been adjusted for age, sex, and baseline pubertal stage. Coefficient of determination (r^2) is calculated as the total sum of squares explained by the model.

Table 5. High-degree nodes (top 5%) in the negative BMI network at baseline for nonfood commercials.

Degree	Degree as proportion of network size[a]	Shen 268 atlas node (Shen et al. 2013)	Region	Canonical network	MNI coordinates (x, y, z)
			Negative network		
25	0.038	246	L Cerebellum	FP	−43, −64, −46
21	0.032	206	L Occipital	VAs	−43, −70, −14
16	0.024	257	White matter (callosal body)	SC	−11, 24, 10
15	0.023	207	L Occipital	VI	−26, −63, −12
15	0.023	200	L Fusiform gyrus	VAs	−43, −52, −17
14	0.021	216	L Lingual gyrus	VI	−22, −67, 7
14	0.021	212	L Occipital	VII	−11, −98, 8
13	0.020	116	R Cerebellum	FP	42, −64, −49
13	0.020	66	R Fusiform gyrus	VAs	46, −60, −15
12	0.018	69	R Fusiform gyrus	VAs	55, −56, −5
11	0.017	261	L Putamen	SC	−25, 6, 0
11	0.017	134	L Orbitofrontal cortex	DMN	−5, 29, −10

[a]Negative network consists of a total of 666 edges.

as well as connections between the SC, VAs, and FP canonical networks.

Two-year follow-up

Functional connectivity networks in response to passive viewing of the “nonfood” commercials did not significantly predict BMI at the 2-year follow-up ($r = 0.115$, nonparametric permutation $P = .117$, $r^2 = 0.015$, MAE = 4.215; Fig. 3f), controlling for age, sex, baseline pubertal stage, and baseline BMI.

Discussion

During adolescence, individuals develop food choice autonomy, forming eating habits and behaviors that continue into adulthood (Videon and Manning 2003, Bassett et al. 2008). Adolescents are exposed to thousands of food commercials increasing their risk of developing unhealthy eating habits that lead to overeating and weight gain (Scully et al. 2012, Zimmerman and Shimoga 2014). In recent meta-analyses, food (vs. nonfood) commercials elicit increased brain activation in regions shown to encode self-control behaviors, modulation of food cravings, reward processing, and visual processing (Yeung 2021, Arrona-Cardoza et al. 2022). However, there is little evidence to understand whether brain network activation patterns to food commercials are associated with future weight change. Here, we observed that a brain network rich in connections in regions previously implicated in stimuli processing and self-control predicted lower current and future BMI. Interestingly, these networks were specific to when the participants were viewing the unhealthy fast-food commercials.

In this investigation, we employed CPM that uses cross-validation to protect against overfitting and ensure that models generalize to novel individuals in the same dataset, increasing the likelihood of replicating the results in novel datasets (Shen et al. 2017). We observed that stronger baseline functional connectivity within subcortical network nodes as well as between subcortical, salience, visual association, and frontoparietal canonical networks was associated with lower BMI at baseline. The most highly interconnected nodes associated with current BMI across all three types of commercials included regions in the fusiform gyrus, hippocampus, and cerebellum (regions assigned in the visual association, subcortical, and frontoparietal canonical networks, respectively), with connections to other visual association, prefrontal, temporal, and subcortical brain regions. We also observed that stronger functional connectivity among regions that encode aspects of memory formation, visual processing, and self-control predicted lower BMI at the 2-year follow-up. The most highly interconnected nodes when predicting lower future BMI included regions in the parahippocampal gyrus and hippocampus, with connections to prefrontal and temporoparietal brain regions. This may suggest that increased interplay among these regions may have a protective effect against the detrimental influences of fast-food marketing on eating behaviors.

The fusiform gyrus was involved in the baseline CPM networks with more connections from this region to inferior frontal gyrus, prefrontal cortex, and caudate being associated with lower baseline BMI. The fusiform gyrus is involved in semantic memory (Mion et al. 2010) but also appears to play a role in the visual processing of food cues in both adults and adolescents (Huerta et al. 2014, van Meer et al. 2015). Children have shown increased bilateral fusiform gyri activation in response to both food and nonfood brand images, while less activation in this area to both food and nonfood brands was associated with greater energy intake of the branded foods (Masterson et al. 2019). The fusiform area, part of the ventral visual pathway, contains subregions with a neural response that is highly selective to images of food (Khosla et al. 2022, Jain et al. 2023). Earlier results (Bruce et al. 2013, Maynard et al. 2017) suggest that the fusiform gyrus might play a more general role in the visual processing of all salient stimuli, both food and nonfood. In agreement with the literature, we corroborate that this is a region implicated in the processing of multiple types of visual cues and highlight that increased functional connectivity of the fusiform gyrus to the frontoparietal and subcortical networks is associated with lower current BMI, a relationship possibly mediated by suppressing the salience of rewarding stimuli commonly shown in fast-food commercials.

The parahippocampal gyrus was a key node in the significant 2-year negative CPM networks with more connections from this region to the prefrontal cortex, orbitofrontal cortex, inferior frontal gyrus, and middle temporal gyrus being linked to lower future BMI. This region plays an important role in memory and learning as well as in the hedonic processing of feeding and encoding of salient stimuli, allowing for food-related recollection (Berthoud 2002, Bragulat et al. 2010). Greater activation in the parahippocampal gyrus correlates with greater food cravings in young women (Chen et al. 2017). Individuals with obesity show increased parahippocampal activation when exposed to naturalistic food odors (Bragulat et al. 2010) and differences in parahippocampal resting-state functional connectivity with increased connections to reward processing regions (Zhang et al. 2020). Furthermore, individuals with obesity show increased activation in the parahippocampal gyrus and decreased activation in the dorsolateral prefrontal cortex during exposure to food images compared to healthy controls (Brooks et al. 2013). In contrast, our results show that stronger connectivity between the parahippocampal gyrus and the prefrontal cortex during viewing of unhealthy fast-food commercials is associated with lower future BMI, suggesting that it is not only the activation within each region that plays a role in the neural processing of food cues but also the connections between different parts of the brain that influence food cue encoding. In this case, strong connections between the parahippocampal gyrus, implicated in cognitive evaluation of salient stimuli, and the prefrontal cortex, implicated in cognitive control, might make individuals to assign a lower motivational value to unhealthy foods shown in commercials and potentially lead to inhibiting consumption of those foods.

A greater number of connections from the hippocampus to prefrontal cortex and inferior frontal gyrus were also linked to both lower current and lower future BMI. The hippocampus, through its involvement in the formation and retrieval of declarative memories (Bird and Burgess 2008), plays a critical role in food intake regulation (Stevenson and Francis 2017) by allowing us to consciously evaluate when, what, and how much to eat. Research suggests that recollection of past eating events acts as a form of self-control to inhibit further food intake (Higgs et al. 2008, Collins and Stafford 2015). Lesions in this area lead to impaired body weight regulation in animal models, suggesting that the hippocampus mediates inhibition of food intake (Davidson et al. 2009, Henderson et al. 2013). During satiation, the hippocampus appears to encode an inhibitory form of learning that allows us to suppress consummatory behaviors despite the presence of pleasant food cues in the environment (Davidson et al. 2009, 2005, 2014). Similarly, human neuroimaging studies have shown that in response to the consumption of a satiating liquid meal, individuals with current and past obesity have decreased regional cerebral blood flow to the hippocampus (DelParigi et al. 2004). Our results are in line with these previous findings and suggest that increased involvement of the hippocampus in frontoparietal, subcortical, motor, and default mode networks is associated with better future weight outcomes. People with obesity have shown reduced BOLD signal intensity in the hippocampus and decreased functional connectivity in the frontal gyrus of the default mode network compared to a control group (Chao et al. 2018), both findings that align with the results presented here. In contrast, BOLD signal intensity in a sample of young adults with obesity was higher in the hippocampus and lower in the prefrontal cortex compared to adults with normal weight, with resting-state activity in the hippocampus mediating task-induced hippocampal activation in response to high-calorie food cues in participants with obesity (Li et al. 2021). Although these results might appear contrasting, they could also suggest the heterogeneity of hippocampal function in the regulation of food intake and the importance of studying whole-brain functional connectivity in parsing out the complex relationships between all the brain networks involved in eating regulation.

It is important to consider the limitations of this study. First, we lacked power to test possible racial/ethnic differences. There is evidence to suggest that Black adolescents are exposed to a higher number of TV ads for snacks and sugary drinks compared to White youth (Miller et al. 2021), placing this group at a greater risk of consuming unhealthier foods. Imaging data for this study were collected in an MRI scanner using an 8-channel head coil, which, compared to the more widely used 32-channel head coil, has shown increased noise amplification and reduced signal-to-noise ratio during data acquisition (Panman et al. 2019). The machine learning approach implemented here provides a more conservative estimate of the strength of the brain–behavior relationship compared to traditional correlation approaches. However, the ultimate test of the generalizability of our results would be whether the predictive networks identified here would relate to body weight measures in an entirely separate sample. Given that we have not performed this external validation, it limits the generalizability and replicability of our results. Additionally, it is important to note that we lacked information on socioeconomic status in this sample. There is evidence to suggest that lower socioeconomic status is associated with altered neural responses to food cues in reward processing and executive control regions (Zhang et al. 2023), with socioeconomic status influencing the relationship between brain food cue reactivity and weight. As such, future studies should include a comprehensive assessment of socioeconomic status. Another variable that would have added further nuance to the results would be recall of the commercials after the fMRI paradigm to assess participants' attention to the task. However, this was not directly tested here. Lastly, over the past several years, there has been a considerable shift from more traditional to digital marketing with the food industry advertising foods and beverages on social media apps, streaming platforms, and video games, with equally alarming effects on children's and adolescents' food choices as traditional TV commercials (Mc Carthy et al. 2022), highlighting the need for further studies.

In sum, this study found that stronger connectivity between regions implicated in memory formation, learning, visual processing, and self-control in response to unhealthy fast-food commercials predicts lower BMI at a 2-year follow-up. These results suggest that some adolescents might be able to exert more self-control over the influence external food stimuli have on their food choices, making them less vulnerable to overeating and weight gain later in life. Further examining the biological and environmental factors that lead to stronger connectivity in this protective network in some individuals could be crucial for understanding the neuropsychological underpinnings of eating behaviors, while longer follow-up studies across developmental transitions would be an important future direction. Although further research on individual-level differences in eating behavior and food choices is warranted, it is imperative to consider the need for population-level changes in policy that strictly regulate fast-food advertisements targeting adolescents.

Acknowledgements

The authors would like to thank the study participants and the research team at the University of Michigan for completion of data collection and initial analyses.

Author contributions

Afroditi Papantoni (Conceptualization; Formal Analysis; Methodology; Visualization; Writing – original draft; Writing – review & editing), Ashley N. Gearhardt (Conceptualization; Funding acquisition; Investigation; Project administration; Resources; Writing

– review & editing), Sonja Yokum (Conceptualization; Investigation; Project administration; Writing – review & editing), Lindzey V. Hoover (Data curation; Writing – review & editing), Emily S. Finn (Conceptualization; Formal Analysis; Methodology; Writing – review & editing), Grace E. Shearrer (Supervision; Writing – review & editing), Lindsey Smith Taillie (Supervision; Writing – review & editing), Saame Raza Shaikh (Supervision; Writing – review & editing), Katie A. Meyer (Supervision; Writing – review & editing), Kyle S. Burger (Conceptualization; Formal Analysis; Methodology; Supervision; Writing – review & editing).

Conflict of interest: None declared.

Funding

This work was supported by the National Institute of Diabetes and Digestive and Kidney Diseases [R01DK102532 (Principal Investigator: A.N.G.)].

Data availability

The imaging data used in the manuscript are publicly available at: https://doi.org/10.7302/5vve-yz30 (Hoover 2022). The code book and analytic code will be made available upon request from the corresponding author.

References

Adise S, Rhee KE, Laurent J *et al*. Limitations of BMI z scores for assessing weight change: a clinical tool versus individual risk. *Obesity* 2024;**32**:445–49. https://doi.org/10.1002/oby.23957

Al-Aidroos N, Said CP, Turk-Browne NB. Top-down attention switches coupling between low-level and high-level areas of human visual cortex. *Proc Natl Acad Sci USA* 2012;**109**:14675–80. https://doi.org/10.1073/pnas.1202095109

Arrona-Cardoza P, Labonté K, Cisneros-Franco JM *et al*. The effects of food advertisements on food intake and neural activity: a systematic review and meta-analysis of recent experimental studies. *Adv Nutr* 2022;**14**:339–51. https://doi.org/10.1016/j.advnut.2022.12.003

Ashburner J. A fast diffeomorphic image registration algorithm. *NeuroImage* 2007;**38**:95–113. https://doi.org/10.1016/j.neuroimage.2007.07.007

Ashburner J, Friston KJ. Unified segmentation. *NeuroImage* 2005;**26**:839–51. https://doi.org/10.1016/j.neuroimage.2005.02.018

Bagnato M, Roy-Gagnon M-H, Vanderlee L *et al*. The impact of fast food marketing on brand preferences and fast food intake of youth aged 10-17 across six countries. *BMC Public Health* 2023;**23**:1436. https://doi.org/10.1186/s12889-023-16158-w

Bassett R, Chapman GE, Beagan BL. Autonomy and control: the co-construction of adolescent food choice. *Appetite* 2008;**50**:325–32. https://doi.org/10.1016/j.appet.2007.08.009

Berthoud H-R. Multiple neural systems controlling food intake and body weight. *Neurosci Biobehav Rev* 2002;**26**:393–428. https://doi.org/10.1016/s0149-7634(02)00014-3

Bird CM, Burgess N. The hippocampus and memory: insights from spatial processing. *Nat Rev Neurosci* 2008;**9**:182–94. https://doi.org/10.1038/nrn2335

Blakemore S-J, Mills KL. Is adolescence a sensitive period for sociocultural processing? *Annu Rev Psychol* 2014;**65**:187–207. https://doi.org/10.1146/annurev-psych-010213-115202

Bonat S, Pathomvanich A, Keil MF *et al*. Self-assessment of pubertal stage in overweight children. *Pediatrics* 2002;**110**:743–47. https://doi.org/10.1542/peds.110.4.743

Boyland EJ, Nolan S, Kelly B *et al*. Advertising as a cue to consume: a systematic review and meta-analysis of the effects of acute exposure to unhealthy food and nonalcoholic beverage advertising on intake in children and adults. *Am J Clin Nutr* 2016;**103**:519–33. https://doi.org/10.3945/ajcn.115.120022

Boyle R, Weng Y. Studying the connectome at a large scale. 2023. https://doi.org/10.31219/osf.io/ay95f

Bragulat V, Dzemidzic M, Bruno C *et al*. Food-related odor probes of brain reward circuits during hunger: a pilot fMRI study. *Obesity* 2010;**18**:1566–71. https://doi.org/10.1038/oby.2010.57

Brooks SJ, Cedernaes J, Schiöth HB. Increased prefrontal and parahippocampal activation with reduced dorsolateral prefrontal and insular cortex activation to food images in obesity: a meta-analysis of fMRI studies. *PLoS One* 2013;**8**:e60393. https://doi.org/10.1371/journal.pone.0060393

Bruce AS, Lepping RJ, Bruce JM *et al*. Brain responses to food logos in obese and healthy weight children. *J Pediatr* 2013;**162**:759–64.e2. https://doi.org/10.1016/j.jpeds.2012.10.003

Burger KS, Stice E. Elevated energy intake is correlated with hyperresponsivity in attentional, gustatory, and reward brain regions while anticipating palatable food receipt. *Am J Clin Nutr* 2013;**97**:1188–94. https://doi.org/10.3945/ajcn.112.055285

Casey BJ, Jones RM. Neurobiology of the adolescent brain and behavior: implications for substance use disorders. *J Am Acad Child Adolesc Psychiatry* 2010;**49**:1189–201. https://doi.org/10.1016/j.jaac.2010.08.017

Chao S-H, Liao Y-T, Chen VC-H *et al*. Correlation between brain circuit segregation and obesity. *Behav Brain Res* 2018;**337**:218–27. https://doi.org/10.1016/j.bbr.2017.09.017

Chen S, Dong D, Jackson T *et al*. Trait-based food-cravings are encoded by regional homogeneity in the parahippocampal gyrus. *Appetite* 2017;**114**:155–60. https://doi.org/10.1016/j.appet.2017.03.033

Cole MW, Ito T, Schultz D *et al*. Task activations produce spurious but systematic inflation of task functional connectivity estimates. *NeuroImage* 2019;**189**:1–18. https://doi.org/10.1016/j.neuroimage.2018.12.054

Collins R, Stafford LD. Feeling happy and thinking about food. Counteractive effects of mood and memory on food consumption. *Appetite* 2015;**84**:107–12. https://doi.org/10.1016/j.appet.2014.09.021

Davidson TL, Chan K, Jarrard LE *et al*. Contributions of the hippocampus and medial prefrontal cortex to energy and body weight regulation. *Hippocampus* 2009;**19**:235–52. https://doi.org/10.1002/hipo.20499

Davidson TL, Kanoski SE, Walls EK *et al*. Memory inhibition and energy regulation. *Physiol Behav* 2005;**86**:731–46. https://doi.org/10.1016/j.physbeh.2005.09.004

Davidson TL, Sample CH, Swithers SE. An application of Pavlovian principles to the problems of obesity and cognitive decline. *Neurobiol Learn Mem* 2014;**108**:172–84. https://doi.org/10.1016/j.nlm.2013.07.014

DelParigi A, Chen K, Salbe AD *et al*. Persistence of abnormal neural responses to a meal in postobese individuals. *Int J Obes Relat Metabol Disord* 2004;**28**:370–77. https://doi.org/10.1038/sj.ijo.0802558

Dietrich A, Hollmann M, Mathar D *et al*. Brain regulation of food craving: relationships with weight status and eating behavior. *Int J Obesity* 2016;**40**:982–89. https://doi.org/10.1038/ijo.2016.28

Douglass AM, Kucukdereli H, Ponserre M *et al.* Central amygdala circuits modulate food consumption through a positive-valence mechanism. *Nat Neurosci* 2017;**20**:1384–94. https://doi.org/10.1038/nn.4623

Farruggia MC, van Kooten MJ, Perszyk EE *et al.* Identification of a brain fingerprint for overweight and obesity. *Physiol Behav* 2020;**222**:112940. https://doi.org/10.1016/j.physbeh.2020.112940

Finn ES, Shen X, Scheinost D *et al.* Functional connectome fingerprinting: identifying individuals using patterns of brain connectivity. *Nat Neurosci* 2015;**18**:1664–71. https://doi.org/10.1038/nn.4135

Finn ES, Bandettini PA. Movie-watching outperforms rest for functional connectivity-based prediction of behavior. *NeuroImage* 2021;**235**:117963. https://doi.org/10.1016/j.neuroimage.2021.117963

Folkvord F, Anschütz DJ, Boyland E *et al.* Food advertising and eating behavior in children. *Curr Opin Behav Sci* 2016;**9**:26–31. https://doi.org/10.1016/j.cobeha.2015.11.016

Frazier WC III, Harris JL. Trends in television food advertising to young people: 2017 update. UConn Rudd Center for Food Policy and Health, 2018.

Gearhardt AN, Yokum S, Stice E *et al.* Relation of obesity to neural activation in response to food commercials. *Soc Cognit Affective Neurosci* 2014;**9**:932–38. https://doi.org/10.1093/scan/nst059

Gearhardt AN, Yokum S, Harris JL *et al.* Neural response to fast food commercials in adolescents predicts intake. *Am J Clin Nutr* 2020;**111**:493–502. https://doi.org/10.1093/ajcn/nqz305

Giuliani NR, Merchant JS, Cosme D *et al.* Neural predictors of eating behavior and dietary change. *Ann NY Acad Sci* 2018;**1428**:208–20. https://doi.org/10.1111/nyas.13637

Greene AS, Gao S, Scheinost D *et al.* Task-induced brain state manipulation improves prediction of individual traits. *Nat Commun* 2018;**9**:2807. https://doi.org/10.1038/s41467-018-04920-3

Harris JL, Sacco SJ, Fleming-Milici F. TV exposure, attitudes about targeted food ads and brands, and unhealthy consumption by adolescents: modeling a hierarchical relationship. *Appetite* 2022;**169**:105804. https://doi.org/10.1016/j.appet.2021.105804

Harris JL. Rudd Center analysis of 2012 Nielsen data. UConn Rudd Center for Food Policy and Health, 2013.

Henderson YO, Smith GP, Parent MB. Hippocampal neurons inhibit meal onset. *Hippocampus* 2013;**23**:100–07. https://doi.org/10.1002/hipo.22062

Higgs S, Williamson AC, Attwood AS. Recall of recent lunch and its effect on subsequent snack intake. *Physiol Behav* 2008;**94**:454–62. https://doi.org/10.1016/j.physbeh.2008.02.011

Hoover LV. Food marketing vulnerability and increased risk for weight gain in adolescents. University of Michigan - Deep Blue Data, 2022.

Huerta CI, Sarkar PR, Duong TQ *et al.* Neural bases of food perception: coordinate-based meta-analyses of neuroimaging studies in multiple modalities. *Obesity* 2014;**22**:1439–46. https://doi.org/10.1002/oby.20659

Jain N, Wang A, Henderson MM *et al.* Selectivity for food in human ventral visual cortex. *Commun Biol* 2023;**6**:175. https://doi.org/10.1038/s42003-023-04546-2

Joshi A, Scheinost D, Okuda H *et al.* Unified framework for development, deployment and robust testing of neuroimaging algorithms. *Neuroinformatics* 2011;**9**:69–84. https://doi.org/10.1007/s12021-010-9092-8

Kelly B, Vandevijvere S, Ng S *et al.* Global benchmarking of children's exposure to television advertising of unhealthy foods and beverages across 22 countries. *Obesity Rev* 2019;**20 Suppl 2**:116–28. https://doi.org/10.1111/obr.12840

Khosla M, Ratan Murty NA, Kanwisher N. A highly selective response to food in human visual cortex revealed by hypothesis-free voxel decomposition. *Curr Biol* 2022;**32**:4159–71.e9. https://doi.org/10.1016/j.cub.2022.08.009

Larsen B, Luna B. Adolescence as a neurobiological critical period for the development of higher-order cognition. *Neurosci Biobehav Rev* 2018;**94**:179–95. https://doi.org/10.1016/j.neubiorev.2018.09.005

Li G, Hu Y, Zhang W *et al.* Resting activity of the hippocampus and amygdala in obese individuals predicts their response to food cues. *Addict Biol* 2021;**26**:e12974. https://doi.org/10.1111/adb.12974

Masterson TD, Stein WM, Beidler E *et al.* Brain response to food brands correlates with increased intake from branded meals in children: an fMRI study. *Brain Imaging Behav* 2019;**13**:1035–48. https://doi.org/10.1007/s11682-018-9919-8

Maynard OM, Brooks JCW, Munafò MR *et al.* Neural mechanisms underlying visual attention to health warnings on branded and plain cigarette packs. *Addiction* 2017;**112**:662–72. https://doi.org/10.1111/add.13699

Mc Carthy CM, de Vries R, Mackenbach JD. The influence of unhealthy food and beverage marketing through social media and advergaming on diet-related outcomes in children—a systematic review. *Obesity Rev* 2022;**23**:e13441. https://doi.org/10.1111/obr.13441

Miller A, Cassidy O, Greene T *et al.* A qualitative analysis of black and white adolescents' perceptions of and responses to racially targeted food and drink commercials on television. *Int J Environ Res Public Health* 2021;**18**:11563. https://doi.org/10.3390/ijerph182111563

Mion M, Patterson K, Acosta-Cabronero J *et al.* What the left and right anterior fusiform gyri tell us about semantic memory. *Brain* 2010;**133**:3256–68. https://doi.org/10.1093/brain/awq272

Noble S, Spann MN, Tokoglu F *et al.* Influences on the test-retest reliability of functional connectivity MRI and its relationship with behavioral utility. *Cereb Cortex* 2017;**27**:5415–29. https://doi.org/10.1093/cercor/bhx230

Noori HR, Cosa Linan A, Spanagel R. Largely overlapping neuronal substrates of reactivity to drug, gambling, food and sexual cues: a comprehensive meta-analysis. *Eur Neuropsychopharmacol* 2016;**26**:1419–30. https://doi.org/10.1016/j.euroneuro.2016.06.013

Nummenmaa L, Hirvonen J, Hannukainen JC *et al.* Dorsal striatum and its limbic connectivity mediate abnormal anticipatory reward processing in obesity. *PLoS One* 2012;**7**:e31089. https://doi.org/10.1371/journal.pone.0031089

Ofcom. Television advertising of food and drink products to children. Ofcom, 2006.

Panman JL, To YY, van der Ende EL *et al.* Bias introduced by multiple head coils in MRI research: an 8 channel and 32 channel coil comparison. *Front Neurosci* 2019;**13**:729. https://doi.org/10.3389/fnins.2019.00729

Pauzé E, Potvin Kent M. Children's measured exposure to food and beverage advertising on television in Toronto (Canada), May 2011-May 2019. *Can J Public Health* 2021;**112**:1008–19. https://doi.org/10.17269/s41997-021-00528-1

Rayner M, Scarborough P, Lobstein T. The UK Ofcom Nutrient Profiling Model. Defining 'Healthy' and 'Unhealthy' Foods and Drinks for TV Advertising to Children. Oxford: Oxford University Press, 2009.

Rosenberg MD, Finn ES, Scheinost D *et al.* A neuromarker of sustained attention from whole-brain functional connectivity. *Nat Neurosci* 2016;**19**:165–71. https://doi.org/10.1038/nn.4179

Rummo PE, Cassidy O, Wells I *et al*. Examining the relationship between youth-targeted food marketing expenditures and the demographics of social media followers. *Int J Environ Res Public Health* 2020;**17**:1631.https://doi.org/10.3390/ijerph17051631

Russell SJ, Croker H, Viner RM. The effect of screen advertising on children's dietary intake: a systematic review and meta-analysis. *Obesity Rev* 2019;**20**:554–68. https://doi.org/10.1111/obr.12812

Scully M, Wakefield M, Niven P *et al*., NaSSDA Study Team. Association between food marketing exposure and adolescents' food choices and eating behaviors. *Appetite* 2012;**58**:1–5. https://doi.org/10.1016/j.appet.2011.09.020

Shen X, Tokoglu F, Papademetris X *et al*. Groupwise whole-brain parcellation from resting-state fMRI data for network node identification. *NeuroImage* 2013;**82**:403–15. https://doi.org/10.1016/j.neuroimage.2013.05.081

Shen X, Finn ES, Scheinost D *et al*. Using connectome-based predictive modeling to predict individual behavior from brain connectivity. *Nat Protoc* 2017;**12**:506–18. https://doi.org/10.1038/nprot.2016.178

Siep N, Roefs A, Roebroeck A *et al*. Fighting food temptations: the modulating effects of short-term cognitive reappraisal, suppression and up-regulation on mesocorticolimbic activity related to appetitive motivation. *NeuroImage* 2012;**60**:213–20. https://doi.org/10.1016/j.neuroimage.2011.12.067

Stevenson RJ, Francis HM. The hippocampus and the regulation of human food intake. *Psychol Bull* 2017;**143**:1011–32. https://doi.org/10.1037/bul0000109

Truman E, Elliott C. Identifying food marketing to teenagers: a scoping review. *Int J Behav Nutr Phys Act* 2019;**16**:67. https://doi.org/10.1186/s12966-019-0833-2

van Meer F, van der Laan LN, Adan RAH *et al*. What you see is what you eat: an ALE meta-analysis of the neural correlates of food viewing in children and adolescents. *NeuroImage* 2015;**104**:35–43. https://doi.org/10.1016/j.neuroimage.2014.09.069

Videon TM, Manning CK. Influences on adolescent eating patterns: the importance of family meals. *J Adolesc Health* 2003;**32**:365–73. https://doi.org/10.1016/s1054-139x(02)00711-5

Yeum D, Jimenez CA, Emond JA *et al*. Differential neural reward reactivity in response to food advertising medium in children. *Front Neurosci* 2023;**17**:1052384. https://doi.org/10.3389/fnins.2023.1052384

Yeung AWK. Brain responses to watching food commercials compared with nonfood commercials: a meta-analysis on neuroimaging studies. *Public Health Nutr* 2021;**24**:2153–60. https://doi.org/10.1017/S1368980020003122

Yip SW, Scheinost D, Potenza MN *et al*. Connectome-based prediction of cocaine abstinence. *Am J Psychiatry* 2019;**176**:156–64. https://doi.org/10.1176/appi.ajp.2018.17101147

Zhang P, Wu G-W, Yu F-X *et al*. Abnormal regional neural activity and reorganized neural network in obesity: evidence from resting-state fMRI. *Obesity* 2020;**28**:1283–91. https://doi.org/10.1002/oby.22839

Zhang X, Wang H, Kilpatrick LA *et al*. Discrimination exposure impacts unhealthy processing of food cues: crosstalk between the brain and gut. *Nat Mental Health* 2023;**1**:841–52. https://doi.org/10.1038/s44220-023-00134-9

Zimmerman FJ, Shimoga SV. The effects of food advertising and cognitive load on food choices. *BMC Public Health* 2014;**14**:342. https://doi.org/10.1186/1471-2458-14-342

Social Cognitive and Affective Neuroscience, 2025, 20(1), nsaf018, DOI: https://doi.org/10.1093/scan/nsaf018, Advance Access Publication Date: 8 March 2025, Original Research & Neuroscience

Received: 6 June 2024; **Revised**: 26 October 2024; **Accepted**: 5 March 2025